Nutrient Dynamics in Flooded Wetlands. I: Model Development

M. M. Hantush, A.M.ASCE[1]; L. Kalin, Ph.D., A.M.ASCE[2]; S. Isik, Ph.D.[3]; and A. Yucekaya[4]

Abstract: Wetlands are rich ecosystems recognized for ameliorating floods, improving water quality, and providing other ecosystem benefits. This part of a two-paper series presents a relatively detailed process-based model for nitrogen and phosphorus retention, cycling, and removal in flooded wetlands. The model captures salient features of nutrient dynamics and accounts for complex interactions among various physical, biogeochemical, and physiological processes. The model simulates oxygen dynamics and the impact of oxidizing and reducing conditions on nitrogen transformation and removal, and approximates phosphorus precipitation and releases into soluble forms under aerobic and anaerobic conditions, respectively. Nitrogen loss pathways of volatilization and denitrification are explicitly accounted for on a physical basis. Processes in surface water and the bottom-active soil layer are described by a system of coupled ordinary differential equations. A finite-difference numerical scheme is implemented to solve the coupled system of ordinary differential equations for various multiphase constituents' concentrations in the water column and wetland soil. The numerical solution algorithm is verified against analytical solutions obtained for simplified transport and fate scenarios. Quantitative global sensitivity analysis revealed consistent model performance with respect to critical parameters and dominant nutrient processes. A hypothetical phosphorus loading scenario shows that the model is capable of capturing the phenomenon of phosphorus precipitation and release under oxic and anoxic conditions, respectively. **DOI: 10.1061/(ASCE)HE.1943-5584.0000741.**

CE Database subject headings: Wetlands; Nitrogen; Phosphorus; Sediment; Nitrification; Denitrification; Ammonia; Oxygen demand; Floods; Nutrients.

Author keywords: Wetlands; Model; Nitrogen; Phosphorus; Sediment; Nitrification; Denitrification; Ammonium; Aerobic; Anaerobic; Sediment oxygen demand; Ammonia volatilization; Diffusion.

Introduction

Wetland ecosystems are transitions between dry lands and aquatic ecosystems which are recognized for their hydrologic, ecological, and economic values (Hammer 1989; Mitsch and Gosselink 2000). Wetlands act as natural purifiers and are known for improving the water quality of industrial waste discharge and urban storm and agricultural runoff. They receive, hold, and recycle nutrients continually washed from urban and agricultural areas. Wetlands provide habitats that support biota and diverse wildlife, and ameliorate floods and recharge aquifers, allowing stored groundwater to sustain base flow in streams during dry periods. They also protect shores against the erosive power of sea waves (Hammer 1989).

Proper management of wetlands and optimizing their hydro-ecological benefits require a quantitative understanding of how these systems function and how they respond to anthropogenic disturbances and alternative management plans (e.g., Brown 1988). Ecological models are useful tools for understanding wetland function and structure, testing hypotheses, and making predictions for decision making.

Wetland processes modeling is fairly recent and a nascent research area (e.g., Mitsch et al. 1988; Min et al. 2011; Walker and Kadleck 2011, on reviews of mechanistic biogeochemical wetland models). Complexities of wetland models describing primary productivity and water quality function vary from the underlying ecosystem addressed by the model to the mathematical system in the model describing a specific wetland ecosystem. Earlier models included empirical relationships relating wetland productivity and biomass growth to hydrology and nutrient inputs (e.g., Bodkin et al. 1972; Mitsch et al. 1988; Odum 1979; Brown 1981; Phipps 1979; Pearlstein et al. 1985), then evolved into simple process-based models with apparent net settling rate or first-order rate reaction/decay (Reed et al. 1988; Watson et al. 1989; Kadlec 1989; Walker 1995; Raghunathan et al. 2001). An improved tier of mechanistic, process-based wetland nutrient and organic carbon models have been developed that account for mass exchange between standing water and wetland soil or biomass compartment [Logofet and Alexandrov 1988; Kadlec and Hammer 1988; Mitsch and Reeder 1991; Water Quality Institute 1992 (MIKE 11 WET); Kadlec 1997; Wang et al. 2009; Paudel et al. 2010]. Among these, the models by Kadlec (1997) and Kadlec and Hammer (1988) are spatially distributed nutrient and biomass models. Paudel and Jawitz (2012) showed that wetland phosphorus model performance improves significantly by accounting for interactive exchanges between overlying water and wetland soil; however, a proposed coefficient of effectiveness and Akaike's information criterion

[1]Senior Scientist, Land Remediation and Pollution Control Division, National Risk Management Research Laboratory, Office of Research and Development, U.S. EPA, 26 W. Martin Luther King Dr., Cincinnati, OH 45268 (corresponding author). E-mail: hantush.mohamed@epa.gov

[2]Associate Professor, School of Forestry and Wildlife Sciences, Auburn Univ., 602 Duncan Dr., Auburn, AL 36849.

[3]Postdoctoral Fellow, School of Forestry and Wildlife Sciences, Auburn Univ., 602 Duncan Dr., Auburn, AL 36849.

[4]Assistant Professor, Industrial Engineering, Kadir Has Univ., Cibali, Istanbul 34083, Turkey.

Note. This manuscript was submitted on March 8, 2012; approved on November 5, 2012; published online on November 7, 2012. Discussion period open until May 1, 2014; separate discussions must be submitted for individual papers. This paper is part of the ***Journal of Hydrologic Engineering***, Vol. 18, No. 12, December 1, 2013. © ASCE, ISSN 1084-0699/2013/12-1709-1723/$25.00.

showed modest improvement with increased model complexity. More complex wetland models that involve a large number of simulated state variables and parameters included those developed by Jørgensen et al. (1988) for fate and transport of nitrogen and phosphorus in three-dimensional variably saturated wetland systems, and the detailed but highly parameterized nutrient models by Brown (1988), Van der Peijl and Verhoeven (1999), and Wang and Mitsch (2000). Computationally intensive, highly nonlinear flow, heat transfer, and Monod-kinetics models have also been used to simulate waste treatment in constructed wetlands, such as the Constructed Wetlands 2 Dimensional (CW2D) model (Langergraber 2001) and the Constructed Wetland Model Number 1 (CWM1) (Langergraber et al. 2009).

Microbial denitrification of nitrate to gaseous forms of nitrogen under anaerobic conditions and their subsequent release to the atmosphere remain one of the more significant ways in which nitrogen is lost from wetland systems (Mitsch and Gosselink 2000). Nitrate introduced with the influent or produced by nitrification is ultimately removed in the anaerobic soil zone typically situated below a thin layer of oxidized soil (a few millimeters to centimeters thick) at the soil surface (e.g., Mitsch and Gosselink 2000). The oxidized soil layer exerts a geochemical control wherein oxidation reactions regulate nitrate production in the process of nitrification which prevents ammonium from further building up in the underlying anaerobic zone.

Ammonia volatilization to the atmosphere is generally less significant, but an important nitrogen loss pathway, especially for pH values greater than 8 (Reddy and Patrick 1984), and it increases with ammonium concentrations in the water column and wind speed (Reddy and Delaune 2008). Up to 70% of nitrogen fertilizers applied to rice paddies can be lost through ammonia volatilization (Reddy and Delaune 2008; Buresh et al. 2008). Linking oxidation and reduction reactions in wetland soils to oxygen dynamics and aerobic-anaerobic wetland soil conditions, and ammonia volatilization to physical and geochemical factors would improve both predictive capability and explanatory depth of existing wetland models to simulate nitrogen transformation and removal. Moreover, such enhancement allows the coupling of oxygen dynamics to precipitation of phosphorus and removal from solution phase under aerobic condition and subsequent release in dissolved form under low oxygen conditions (e.g., Mitsch and Gosselink 2000; Di Toro 2001). The objective of this paper is to improve the dynamics of nutrient retention, removal, and cycling in flooded wetlands and develop a computationally simple nutrient wetland model given the details of processes being modeled. The model is unique in a sense that it (1) simulates with relative ease the dynamics of the thickness of the soil surface aerobic layer and nitrogen transformation and removal on the basis of oxygen dynamics in the wetland system; (2) accounts for ammonia volatilization losses as a function of physicochemical parameters; and (3) simulates approximately the phenomenon of phosphorus precipitation under oxidized conditions and release into solution under anoxic conditions.

This manuscript formulates and quantitatively examines the wetland nutrient model. In Paper II (Kalin et al. 2013), the model is applied to a restored treatment wetland to evaluate nutrient removal and examine its ability to capture the key nutrient dynamics at the study site. In the following sections, the conceptual model is described, and the mathematical model is presented. Model parameters are presented or derived in terms of climate and environmental parameters. The numerical solver is presented and verified by comparison with analytical solutions, and quantitative global sensitivity analysis is conducted to examine model consistency. A scenario application is carried out to illustrate model capability to simulate the phenomenon of orthophosphate precipitation and release and the dependence of this phenomenon on oxygen concentration variations and local flow conditions. The manuscript ends with a summary and conclusions.

Model Development

Conceptual Model

Figs. 1 and 2 depict the conceptual model for complete biogeochemical pathways of mineralization of organic matter to ammonia and phosphate and subsequent transport, retention, uptake, and removal (denitrification, volatilization, and burial) in flooded wetlands. The model partitions a wetland into three basic compartments: (1) water column (free water), (2) wetland soil layer, and (3) plant biomass. The soil layer is further partitioned into aerobic and anaerobic zones (Faulkner and Richardson 1989; Mitsch and Gosselink 2000). The aerobic layer at the soil-water interface is not a fixed layer, and its thickness is determined by the supply of oxygen to the soil surface and consumption of oxygen in the soil (Reddy and Delaune 2008).

For the sole purpose of simplicity, particulate organic nitrogen is modeled independent of the redox conditions (i.e., aerobic and anaerobic) in wetland soils, with slowly (stable) and fast (labile) decomposing (mineralizing) fractions. A clear break in fast and slowly decomposing plant biomass, and hence, mineralization rates have been reported by Reddy and Delaune (2008). Inert (refractory) organic nitrogen fraction is accounted for by assuming that the sum of slowly and fast-reacting fractions is less than one. The interactions between the free-water and soil compartments occur as a result of settling and resuspension of particulate matter, and advective and diffusive mass exchange of dissolved constituents. Burial is caused by net sedimentation, whereby dissolved and particulate constituents appear advecting downward relative to a moving interface (Di Toro 2001). In natural wetlands, burial is a potential loss pathway that may have a long-term impact on mass balance (e.g., at the annual time scale or decades).

Sources of ammonia and nitrate to the wetland water column include agricultural and urban runoff, groundwater discharge, mineralization of suspended organic nitrogen, sediment feedback (diffusion and resuspension), and atmospheric depositions. Although they might play a minor role in constructed wetlands, atmospheric deposition and nitrogen gas (N_2) fixation are major inputs for bogs in the northeast (Hammer 1989). Nitrification of ammonium nitrogen occurs in the aerobic part of the soil and the water column, whereas nitrate removal by denitrification is confined to the underlying anaerobic zone of the active soil layer. Nitrification also occurs near roots in the rhizosphere of wetland plants and can be as significant as at the soil surface (Kirk and Kronzucker 2005). Dissociation of NH_4^+ into ammonia gas (NH_3) and subsequent volatilization to the atmosphere is a significant loss pathway for nitrogen under conditions of high alkalinity (Reddy and Delaune 2008). In addition to influent concentrations, nitrate (NO_3^-) is produced by oxidation of ammonium ion (NH_4^+) in the water column and oxidized soil layer.

Unlike nitrogen, phosphorus follows the sediment pathways of sedimentation and resuspension with no gaseous losses (Mitsch and Gosselink 2000). The physical processes of advection (inflow, outflow), settling, resuspension, and diffusion similarly apply to inorganic phosphorus transport and fate in the wetland water. Only the biologically available inorganic phosphorus (typically orthophosphate) is available for uptake by plants. For simplicity, the binding of phosphorus (orthophosphate) in organic matter and adsorption onto mineral soil particles are modeled here with the linear

J. Hydrol. Eng., 2013, 18(12): 1709-1723

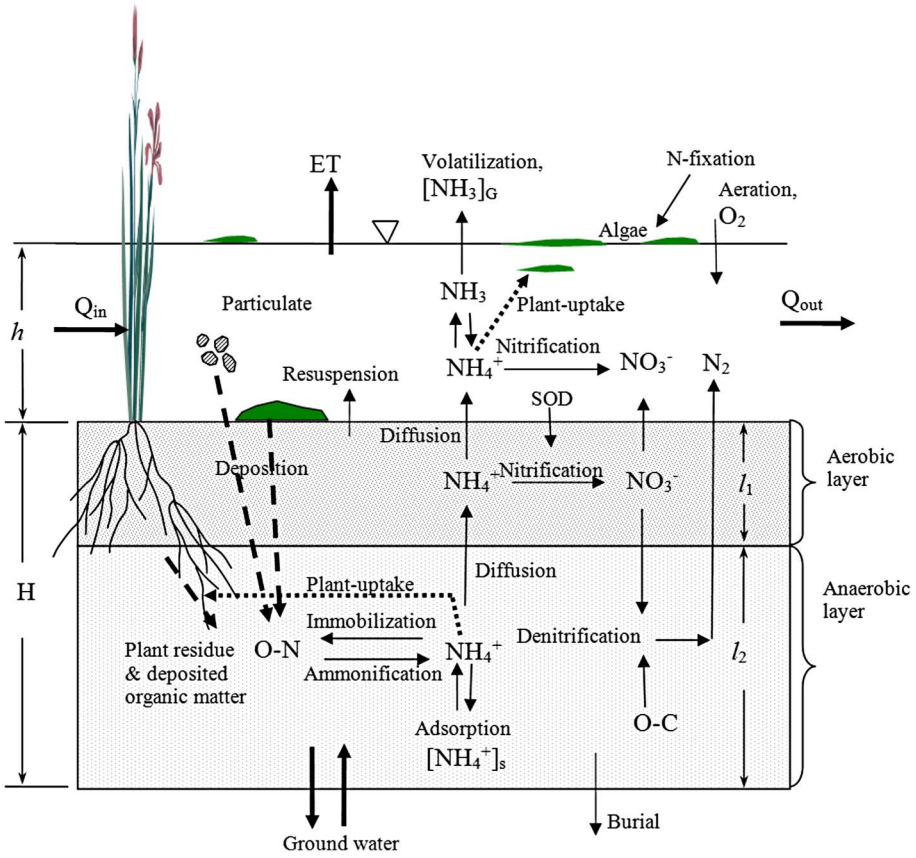

Fig. 1. Nitrogen processes in wetlands: water column, aerobic soil layer, and reduced lower soil layer

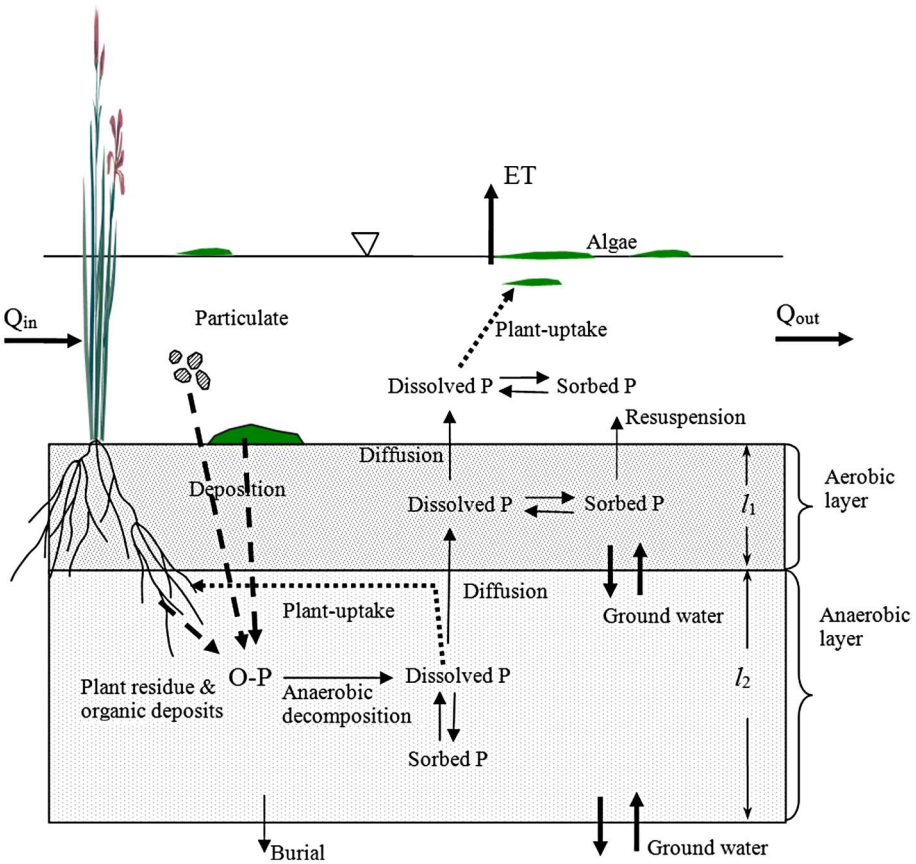

Fig. 2. Phosphorus processes in wetlands: water column, aerobic soil layer, and lower reduced soil layer

J. Hydrol. Eng., 2013, 18(12): 1709-1723

adsorption isotherm. Imported phosphorus (runoff, sediment, groundwater) and decomposition of organic matter are primary sources of inorganic phosphorus in wetland soil and water. Excluding plant harvesting, burial is about the only mechanism for the removal of phosphorus in wetlands.

As discussed above, the removal of dissolved orthophosphate from solution occurs under oxidized soil conditions, whereby phosphorus bonds with precipitating iron hydroxide and separates from solution. When oxygen levels drop, the iron hydroxides are reduced to soluble ferrous iron, which leads to an associated release of dissolved phosphorus into the sediment pore waters where it is free for transport into the overlying water (e.g., Mitsch and Gosselink 2000; Di Toro 2001).

Although the primary objective of the wetland model is nutrient cycling, productivity is modeled using a generic mass balance for free-floating algae and rooted plants with relatively simple growth and death processes. Major underlying assumptions of the wetland model are as follows: (1) concentrations of various constituents are uniform (i.e., complete mixing) in each compartment or layer; (2) first-order reaction rates occur (mineralization, nitrification, denitrification, etc.); (3) abundant dissolved organic carbon (DOC) is present in soil; (4) the aerobic layer is aggregate (i.e., effective layer) of the oxidizing soil surface and the rhizosphere; (5) phosphorus precipitation and release could be approximated by an oxygen-dependent linear adsorption coefficient; and (6) nitrogen fixation and assimilation into microbial biomass are accounted for in the organic pool. The consequence of unlimited DOC supply in the third of the above assumptions is that denitrification would not be limited by DOC. If the supply of DOC is limited, a more rigorous approach would require the coupling of nitrate and DOC dynamics, e.g., with Monod kinetics describing the rate of denitrification. Assumption (6) follows from neglecting microbial growth and decay as a separate compartment; i.e., nitrogen fixed by or assimilated into microbial biomass is at equilibrium with the amount released to the organic pool. Extension of the model to multiple cells arranged in series along the main flow direction is straightforward for applications involving spatially variable data.

Wetland Model Equations

Figs. 1 and 2 depict various transport mechanisms and loss pathways for nitrogenous species and phosphorus in both free-water and sediment compartments in a typical flooded wetland system. These are accounted for in the mass balance ordinary differential equations that are presented below. First, we start with the hydrologic model.

Water Flow

Surface flow routing in a wetland system can be described using a simple flow continuity equation:

$$\phi_w \frac{dV_w}{dt} = Q_i + Q_g - Q_o - AE_T + Ai_p \tag{1}$$

where V_w is the water volume of wetland surface water [L^3]; A is the wetland surface area [L^2]; Q_i is the volumetric inflow rate [L^3T^{-1}]; Q_g is groundwater discharge (negative for infiltration) [L^3T^{-1}]; Q_o is wetland discharge (outflow) rate [L^3T^{-1}]; i_p is precipitation rate [LT^{-1}]; E_T is evapotranspiration rate [$L^3T^{-1}L^{-2}$]; and ϕ_w is effective porosity of wetland surface water (since biomass occupies part of the submerged wetland volume). E_T accounts for the wetland evapotranspiration rate [$L^3T^{-1}L^{-2}$] which is the sum of plant transpiration (T_r) and surface evaporation (E_v), $E_T = T_r + E_v$. Although T_r is derived by plant uptake in the soil root zone, it is accounted for in the E_T term to maintain appropriate mass balance for the entire wetland system (free water and soil). By lumping plant transpiration rate into the surface reservoir flow balance, flow balance for the overall wetland system is maintained but without the need to compute T_r.

The outflow-depth relationship (rating-curve) of the form $Q_o = \rho h^{\varepsilon}$, where $h = \phi_w V_w/A$, can be used to route flow out of the wetland for a given inflow event, Q_i. The specific case of $\varepsilon = 1$ corresponds to a linear-reservoir model.

Nitrogen

Mass balance of nitrogen constituents in the water column is described by the following ordinary differential equations:

$$\begin{aligned}\phi_w \frac{d(V_w N_{ow})}{dt} &= Q_i N_{owi} + a_{na} k_{da} a + a_{na} k_{db} f_{bw} b \\ &\quad - \phi_w V_w k_{mw} N_{ow} - v_s \phi_w A N_{ow} \\ &\quad + v_r \phi_w A (N_{or} + N_{os}) - Q_o N_{ow} + A f_{Sw} S\end{aligned} \tag{2}$$

$$\begin{aligned}\phi_w \frac{d(V_w N_{aw})}{dt} &= Q_i N_{awi} + i_p A N_{ap} - \phi_w V_w f_N k_{nw} N_{aw} \\ &\quad + \beta_{a1} A (N_{a1} - N_{aw}) + F^w_{N_a g} \\ &\quad - k_v \phi_w A (1 - f_N) N_{aw} + \phi_w V_w k_{mw} N_{ow} \\ &\quad - Q_o N_{aw} - f_{aw} a_{na} k_{ga} a + A q_a\end{aligned} \tag{3}$$

$$\begin{aligned}\phi_w \frac{d(V_w N_{nw})}{dt} &= Q_i N_{nwi} + i_p A N_{np} + \phi_w V_w f_N k_{nw} N_{aw} \\ &\quad + \beta_{n1} A (N_{n1} - N_{nw}) + F^w_{N_n g} - f_{nw} a_{na} k_{ga} a \\ &\quad - Q_o N_{nw} + A q_n\end{aligned} \tag{4}$$

in which

$$k_{nw} = k^*_{nw}(1 - e^{-\lambda_w O_w}) \tag{5}$$

$$F^w_{xg} = \begin{cases} Q_g x_1, & Q_g > 0 \\ Q_g x_w, & Q_g < 0 \end{cases}, \qquad x{:}N_a, N_n \tag{6}$$

where N_{ow} is particulate organic nitrogen concentration in free water [ML^{-3}]; $N_{aw} = [NH_4^+] + [NH_3]$ is total ammonia-nitrogen concentration in free water [ML^{-3}]; N_{nw} is nitrate-nitrogen concentration in free water [ML^{-3}]; O_w is oxygen concentration in free water [ML^{-3}]; a is mass of free floating plant [M *Chl a*]; b is mass of rooted plants [M *Chl a*]; N_{owi}, N_{awi}, and N_{nwi}, respectively, are concentrations of organic nitrogen, total ammonia nitrogen, and nitrate nitrogen in incoming inflow [ML^{-3}]; N_{a1} and N_{n1}, respectively, are pore-water concentrations of total ammonia nitrogen and nitrate nitrogen in oxygenated top soil layer (aerobic layer in Figs. 1 and 2) [ML^{-3}]; N_{or} is concentration of rapidly mineralizing organic nitrogen in wetland soil [ML^{-3}]; N_{os} is the concentration of slowly mineralizing organic nitrogen in wetland soil [ML^{-3}]; N_{ap} and N_{np}, respectively, are concentrations of total ammonia nitrogen and nitrate nitrogen in precipitation [ML^{-3}]; q_a and q_n, respectively, are dry depositional rates of total ammonia nitrogen and nitrate [$ML^{-2}T^{-1}$]; v_s is effective settling velocity [LT^{-1}]; v_r is resuspension rate [LT^{-1}]; S is rate of nitrogen fixation by microorganisms [$ML^{-2}T^{-1}$]; $F^w_{N_a g}$ and $F^w_{N_n g}$, respectively, are groundwater source/loss for total ammonia nitrogen and nitrate nitrogen [MT^{-1}]; and f_N is the fraction of total ammonia in ionized form. All other related physical, biochemical, reaction, and physiological parameters are defined in the notation list.

Eq. (5), proposed first by Brown and Barnwell (1987), later cited by Chapra (1997), limits the nitrification rate to oxygen levels

J. Hydrol. Eng., 2013, 18(12): 1709-1723

in the water column. In this equation, λ_w is the first-order nitrification inhibition coefficient (≈ 0.6 L mg^{-1}) that can be adjusted during calibration.

Eq. (3) is obtained by expressing the mass balance equation for ammonium ions (NH_4^+) and ammonia (NH_3) individually and recognizing the equilibrium dissociation reaction: $NH_4^+ \leftrightarrow NH_3 + H^+$. The sum of the two equations should yield Eq. (3) (see Chapra 1997; Hantush 2007). In this equation, the term $(1 - f_N)$, which is the fraction of total ammonia in un-ionized form, appears because volatilization is limited to un-ionized ammonia (NH_3). An empirical equation relating f_N to pH and temperature is given in Appendix II [Eq. (47)], and the dependence on temperature of all other biochemical parameters is also included in Appendix II. In Appendix I, we derive a relationship between ammonia volatilization rate k_v and wind speed (U_w) using a two-film resistance model and known relationships between liquid-film and gaseous-film exchange coefficients (Chapra 1997; Jørgensen and Bendoricchio 2001):

$$k_v = \frac{1.17\alpha}{1 + 12.07\alpha U_w^{\eta-1}} U_w^{\eta} \tag{7}$$

where α and η are empirical parameters. In Eq. (7) both U_w and k_v are in md^{-1}. For example, for open-water bodies such as lakes, $\alpha = 0.864$ (Chapra 1997 citing Broecker et al. 1978) and $\eta = 1$. Due to the wind-shielding nature of green cover, it might be reasonable to assume that $\alpha < 0.864$. Note that the product $k_v(1 - f_N)$ on the left-hand side of Eq. (3) could be interpreted as the effective volatilization rate velocity (of total ammonia nitrogen), which is a function of measurable environmental and climate parameters, as well as two empirical parameters. Wang et al. (2009) considered dependence of k_v on temperature and pH, whereas the volatilization rate expression $k_v(1 - f_N)$ accounts for wind speed in addition to the above two parameters (Reddy and Delaune 2008).

Mass balance of particulate organic nitrogen in the soil is given by the following equations:

$$V_s \frac{dN_{or}}{dt} = f_r a_{na} k_{db} f_{bs} b + f_r v_s \phi_w A N_{ow} - v_r \phi_w A N_{or} - V_s k_{mr} N_{or} - v_b A N_{or} + f_r (1 - f_{Sw}) A S \tag{8}$$

$$V_s \frac{dN_{os}}{dt} = f_s a_{na} k_{db} f_{bs} b + f_s v_s \phi_w A N_{ow} - v_r \phi_w A N_{os} - V_s k_{ms} N_{os} - v_b A N_{os} + f_s (1 - f_{Sw}) A S \tag{9}$$

where N_{or} and N_{os} are defined above; v_b is the burial velocity [LT^{-1}]; $V_s = H\,A$ is the volume of the active sediment layer [L^3]; and H is the thickness of the active soil layer [L]. (Refer to the notation list for definitions of all other physical and biochemical parameters/coefficients.)

In the aerobic soil layer, mass balance of nitrogen is described by the following equations:

$$\phi V_1 R_s \frac{dN_{a1}}{dt} = -A\beta_{a1}(N_{a1} - N_{aw}) + F^1_{N_a g} - f_{a1} a_{na} k_{gb} f_1 b - \phi A v_b N_{a1} - \phi V_1 f_N k_{ns} N_{a1} + A\beta_{a2}(N_{a2} - N_{a1}) + V_1 k_{mr} N_{or} + V_1 k_{ms} N_{os} \tag{10}$$

in which

$$R_s = 1 + \frac{m_s K_d f_N}{\phi} \tag{11}$$

$$k_{ns} = k^*_{ns}(1 - e^{-\lambda_s O_w}) \tag{12}$$

and

$$\phi V_1 \frac{dN_{n1}}{dt} = -A\beta_{n1}(N_{n1} - N_{nw}) + F^1_{N_n g} + \phi V_1 f_N k_{ns} N_{a1} - A\beta_{n2}(N_{n1} - N_{n2}) - f_{n1} a_{na} k_{gb} f_1 b - v_b \phi A N_{n1} \tag{13}$$

in which

$$F^1_{xg} = \begin{cases} Q_g x_2 - Q_g x_1, & Q_g > 0 \\ Q_g x_1 - Q_g x_w, & Q_g < 0 \end{cases}, \qquad x{:}N_a, N_n \tag{14}$$

where V_1 is the volume of aerobic soil [L^3]; R_s is the total ammonia retardation factor in wetland soil; ϕ is wetland soil porosity; N_{a2} is the total ammonia-nitrogen pore-water concentration in the lower anaerobic layer [ML^{-3}]; N_{n2} is the nitrate-nitrogen pore-water concentration in the lower anaerobic layer [ML^{-3}]; $f_1 = l_1/(l_1 + l_2)$ is the volumetric fraction of the aerobic soil layer; l_1 is the thickness of the aerobic soil layer [L]; l_2 is the thickness of the anaerobic soil layer [L]; $F^1_{N_a g}$, $F^1_{N_n g}$, are, respectively, groundwater source/loss of total ammonia nitrogen and nitrate in the aerobic layer [MT^{-1}]; and m_s is the soil bulk density [ML^{-3}]. Refer to the notation list for all other physical and biochemical parameters.

Nitrogen mass balance in the anaerobic soil layer is

$$\phi V_2 R_s \frac{dN_{a2}}{dt} = -A\beta_{a2}(N_{a2} - N_{a1}) - \phi A v_b (N_{a2} - N_{a1}) + F^2_{N_a g} + V_2 k_{mr} N_{or} + V_2 k_{ms} N_{os} - f_{a2} a_{na} k_{gb} f_2 b \tag{15}$$

$$\phi V_2 \frac{dN_{n2}}{dt} = A\beta_{n2}(N_{n1} - N_{n2}) - \phi V_2 k_{dn} N_{n2} - \phi A v_b (N_{n2} - N_{n1}) + F^2_{N_n g} - f_{n2} a_{na} k_{gb} f_2 b \tag{16}$$

in which

$$F^2_{xg} = \begin{cases} Q_g x_G - Q_g x_2, & Q_g > 0 \\ Q_g x_2 - Q_g x_1, & Q_g < 0 \end{cases}, \qquad x{:}N_a, N_n \tag{17}$$

where N_{aG} is the total ammonia-nitrogen concentration in groundwater [ML^{-3}]; N_{nG} is the nitrate-nitrogen concentration in groundwater [ML^{-3}]; $f_2 = l_2/(l_1 + l_2)$ is the volumetric fraction of the reduced soil layer; V_2 is the volume of anaerobic soil [L^3]; and $F^2_{N_a g}$, $F^2_{N_n g}$ are groundwater source/loss of total ammonia nitrogen and nitrate in the anaerobic layer [MT^{-1}]. Refer to the notation list for definitions of other parameters/coefficients.

Sediment Dynamics

Sediment transport and fate in wetland water may be described by

$$\phi_w \frac{d(V_w m_w)}{dt} = Q_i m_{wi} - v_s \phi_w A m_w + v_r \phi_w A m_s - Q_o m_w \tag{18}$$

Mass balance in the active soil compartment is given by

$$V_s \frac{dm_s}{dt} = v_s \phi_w A m_w - v_r \phi_w A m_s - v_b A m_s \tag{19}$$

where m_w is the sediment concentration in free water [ML^{-3}]; m_{wi} is the sediment concentration in incoming flow [ML^{-3}]; $m_s = (1 - \phi)\rho_s$ is the wetland soil bulk density [ML^{-3}]; and ρ_s is the soil particle density [ML^{-3}].

For convenience, we assume steady-state sediment concentration and drop its time-derivative from Eq. (19); this is equivalent to stating that ϕ and ρ_s are not changing with time.

Oxygen Dynamics in Water Column

Oxygen variations in the water column can be described by

J. Hydrol. Eng., 2013, 18(12): 1709-1723

$$\phi_w \frac{d(V_w O_w)}{dt} = Q_i O_{wi} + i_p A O_p + K_o \phi_w A(O^* - O_w) - r_{on,m}\phi_w V_w k_{mw} N_{ow} - r_{on,n}\phi_w V_w f_N k_{nw} N_{aw} + a_{oc} r_{c,chl}\{(k_{gb} - k_{db}) f_{bw} b + (k_{ga} - k_{da}) a\} - Q_o O_w - A S_O - \phi_w V_w S_w - E_T A O_w \quad (20)$$

where O_{wi} is the concentration of oxygen in incoming water [ML^{-3}]; O_p is the concentration of total oxygen in precipitation [ML^{-3}]; O^* is the oxygen concentration in the air (assumed at saturation) [ML^{-3}]; K_o is the oxygen mass-transfer coefficient [LT^{-1}] [e.g., $K_o = 0.864\ U_w$, where U_w is wind speed (md^{-1}), Broecker et al. (1978)]; S_O is the wetland soil oxygen depletion rate per unit area [$ML^{-2}T^{-1}$]; and S_w is the volumetric oxygen consumption rate in water by other processes [$ML^{-3}T^{-1}$]. Also, refer to the notation list for other parameters/coefficients.

Oxygen Penetration in Wetland Soil

Using the equivalence of two-film theory and assuming a linear drop of oxygen concentration from the ambient level O_w to zero at depth l_1 below the soil surface, conservation of oxygen mass flux across the soil-water interface yields the following expression modified for constricted (porous) wetland surface water (Hantush 2007):

$$S_O = \phi\tau D_o^* \frac{O_w}{l_1 + \frac{\phi\tau}{\phi_w \tau_w}\delta} \quad (21)$$

where δ is the thickness of a laminar (diffusive) boundary layer situated on top of the soil-water interface [L]; τ is the wetland soil tortuosity factor; τ_w is effective tortuosity of the flooded area above soil; and D_o^* is the free-water oxygen diffusion coefficient [L^2T^{-1}]. The typical thickness of the diffusive boundary layer, δ, in natural waters (streams, lakes, oceans) is of the order of millimeters. For slowly flowing and shallow wetland waters, the boundary layer is relatively thicker, and δ might be approximated as half the free-water depth, $\delta \approx h/2$.

We relate oxygen consumption in the aerobic layer to the processes of nitrification, aerobic decomposition of organic matter (mineralization), and allow for other but unknown sinks. Conservation of oxygen mass in wetland soil requires

$$S_O = l_1 r_{on,n}\phi f_N k_{ns}(O_w) N_{a1} + l_1 r_{on,m}(k_{ms} N_{os} + k_{mr} N_{or}) + l_1 S_s \quad (22)$$

where S_s is the oxygen removal rate per unit volume of aerobic layer by other processes.

Let

$$\Omega = r_{on,n}\phi f_N k_{ns}(O_w) N_{a1} + r_{on,m}(k_{ms} N_{os} + k_{mr} N_{or}) + S_s \quad (23)$$

Eqs. (21) and (22) can be combined and solved for l_1 to yield

$$l_1 = -\phi\tau\delta + \sqrt{(\phi\tau\delta)^2 + 2\phi\tau D_o^* O_w/\Omega} \quad (24)$$

This equation constitutes the basis for estimating the thickness of the aerobic sediment layer. For the simple case of $\delta = 0$, Eq. (24) reduces to $l_1 = \sqrt{2\phi\tau D_o^* O_w/\Omega}$.

The significance of Eq. (24) is obvious; it defines the thickness of the top oxic soil layer where nitrification occurs and nitrate is produced. Once l_1 is computed from Eq. (24) for an active sediment layer of thickness H, the thickness of the lower anoxic layer wherein denitrification occurs would therefore be $l_2 = H - l_1$. However, l_1 is typically much smaller than l_2 (varies from a few millimeters to 1–2 cm) (Reddy and Delaune 2008), thus, $l_2 \approx H$.

Phosphorus

Mass balance of phosphorus in the water column may be described by the following ordinary differential equation:

$$\frac{d(V_w P_w)}{dt} = Q_i P_{wi} - v_s F_{sw} m_w \phi_w A P_w + f_1 v_r \phi_w A F_{ss} m_s P_1 + f_2 v_r \phi_w A f_{ss} m_s P_2 - a_{pa} k_{ga} a + V_w a_{pn} k_{mw} N_{ow} + \beta_{p1} A(F_{ds} P_1 - F_{dw} P_w) + F_{Pg}^w - Q_o P_w \quad (25)$$

in which

$$F_{dw} = \frac{1}{1 + K_w m_w}, \qquad F_{sw} = \frac{K_w}{1 + K_w m_w},$$
$$F_{ds} = \frac{1}{\phi + (1-\phi)\rho_s K_{s1}}, \qquad F_{ss} = \frac{K_{s1}}{\phi + (1-\phi)\rho_s K_{s1}},$$
$$f_{ss} = \frac{K_{s2}}{\phi + (1-\phi)\rho_s K_{s2}} \quad (26)$$

$$F_{Pg}^w = \begin{cases} Q_g F_{ds} P_1, & Q_g > 0 \\ Q_g F_{dw} P_w, & Q_g < 0 \end{cases} \quad (27)$$

where P_w is the total inorganic phosphorus concentration in free water [ML^{-3}]; P_{wi} is the inflow total inorganic phosphorus concentration [ML^{-3}]; P_1 is the total phosphorus concentration in the aerobic layer [ML^{-3}]; P_2 is the total phosphorus concentration in the anaerobic layer [ML^{-3}]; F_{Pg}^w is the net advective groundwater contribution of total inorganic phosphorus to the aerobic layer [MT^{-1}]; $F_{d,w}$ is the dissolved fraction of total inorganic phosphorus in free water; $m_w F_{s,w}$ is the sorbed fraction of total inorganic phosphorus in free water ($1 - F_{d,w}$); $\phi F_{d,s}$ is the dissolved fraction of total inorganic phosphorus in the aerobic layer; $m_s F_{s,s}$ is the sorbed fraction of total inorganic phosphorus in the aerobic layer; K_{s1} is the distribution coefficient in the aerobic layer [L^3M^{-1}]; $m_s f_{s,s}$ is the sorbed fraction of the total inorganic phosphorus concentration in the anaerobic layer; and K_{s2} is the distribution coefficient in reduced wetland soil [L^3M^{-1}].

The sorption coefficients in Eqs. (26) and (29) are obtained by noting that $P_w = p + m_w s$ in the water column and $P = \phi p + m_s s$ in the soil (volume averaged, i.e., residence concentration), where p is the dissolved phosphorus concentration [ML^{-3}]; $s = Kp$ is the adsorbed phosphorus concentration [MM^{-1}]; and K is the sorption coefficient (K_w, K_{s1}, and K_{s2}) [L^3M^{-1}].

Rather than limiting resuspended phosphorus to the top aerobic soil compartment, Eq. (25) allows resuspension of sediment-bound phosphorus from the entire active soil layer. Each of the soil compartments contributes an amount proportional to its respective thickness. This is intuitive because resuspension is a purely hydrodynamic process independent of the soil redox condition.

In the aerobic soil layer, mass balance of phosphorus is given by:

$$V_1 \frac{dP_1}{dt} = f_1 \phi_w A v_s m_w F_{sw} P_w - f_1 \phi_w A v_r m_s F_{ss} P_1 - \beta_{p1} A(F_{ds} P_1 - F_{dw} P_w) - v_b A P_1 + \beta_{p2} A(f_{ds} P_2 - F_{ds} P_1) + F_{Pg}^1 - a_{pa} k_{gb} f_1 b + V_1 a_{pn} k_{mr} N_{or} + V_1 a_{pn} k_{ms} N_{os} \quad (28)$$

in which

$$f_{ds} = \frac{1}{\phi + (1-\phi)\rho_s K_{s2}} \quad (29)$$

$$F_{Pg}^1 = \begin{cases} Q_g f_{ds} P_2 - Q_g F_{ds} P_1, & Q_g > 0 \\ Q_g F_{ds} P_1 - Q_g F_{dw} P_w, & Q_g < 0 \end{cases} \quad (30)$$

J. Hydrol. Eng., 2013, 18(12): 1709-1723

where F^1_{Pg} is the net advective groundwater contribution of total phosphorus to the aerobic layer [MT^{-1}]; and $\phi f_{d,s}$ is the dissolved fraction of total phosphorus concentration in the anaerobic soil layer.

Mass balance of phosphorus in the anaerobic layer is given by

$$V_2\frac{dP_2}{dt} = f_2\phi_w A v_s m_w F_{sw} P_w - f_2\phi_w A v_r m_s f_{ss} P_2 + V_2 a_{pn} k_{mr} N_{or} + V_2 a_{pn} k_{ms} N_{os} - v_b A(P_2 - P_1) - \beta_{p2} A(f_{ds}P_2 - F_{ds}P_1) + F^2_{Pg} - a_{pa} k_{gb} f_2 b \quad (31)$$

where

$$F^2_{Pg} = \begin{cases} Q_g P_g - Q_g f_{ds} P_2, & Q_g > 0 \\ Q_g f_{ds} P_2 - Q_g F_{ds} P_1, & Q_g < 0 \end{cases} \quad (32)$$

Similarly, the preceding equations assumed that the aerobic and anaerobic soil compartments receive sediment-bound phosphorus depositional fluxes in proportion to their respective thicknesses [first terms on the right-hand side of Eqs. (28) and (31)].

Phosphorus Adsorption and Precipitation

We account in an approximate fashion for the aggregate effect of sorption onto precipitated iron hydroxide under aerobic conditions and release into solution when anoxic conditions prevail with a proposed functional relationship. The precipitation of phosphorus and release into aqueous phase could be accounted for by artificially increasing or decreasing the distribution coefficient according to oxygen levels in the bulk water. Thus, we relate the sorption rate in the aerobic layer to the oxygen level in the overlying water by suggesting the following functional relationship:

$$K_{s1} = K_{sa} + K_{sb}\frac{O_w}{O^*}, \qquad O_w \le O^*$$
$$K_{s1} = K_{sa} + K_{sb}, \qquad O_w > O^* \quad (33)$$

where K_{sa} accounts for partitioning to phosphorus sorption sites [L^3M^{-1}]; and K_{sb} accounts for association with the iron hydroxide precipitate [L^3M^{-1}]. This relationship predicts $K_{s1} = K_{sa}$ when $O_w = 0$, whereas $K_{s1} = K_{sa} + K_{sb}$ when $O_w = O^*$. K_{s1} could be thought of as an effective distribution coefficient, wherein K_{sb} is treated as a calibration parameter. In general, the oxygen concentration threshold value in Eq. (33), O^*, might be selected smaller than the oxygen saturation concentration.

A more general extension to Eq. (33) is $K_{s1} = K_{sa} + K_{sb}(1 - e^{-cO_w})$, which for $cO_w \ll 1$ can be approximated as $K_{s1} = K_{sa} + K_{sb}\{1 - [1 - (-cO_w) - O(cO_w)^2]\} \cong K_{sa} + K_{sb}cO_w$. Note the similarity with Eq. (33) with $c = (O^*)^{-1}$.

Primary Productivity Model

We use a simple mass balance model for plant biomass growth and death (e.g., Thoman and Mueller 1987; Chapra 1997), and separate free-floating plant biomass (e.g., phytoplankton) from rooted aquatic plants and those attached to the sediment mat (e.g., benthic algae). As indicated earlier, microbial biomass growth and death are not modeled, and nutrients assimilated are assumed to be released instantly to the organic matter pool. A more rigorous approach, of course, is to model this process with nitrogen and phosphorus assimilated (immobilization and nitrogen fixation) into a separate microbial biomass compartment and with subsequent releases upon death/excretion.

We present a simple model for productivity in which the daily growth rate is related to daily solar radiation and the annual growth rate of plants. The MIKE 11 WET model uses a similar concept but with plant uptake rather than growth rate-solar radiation relationship.

The equation governing rooted/benthic plant growth/death is

$$\frac{db}{dt} = k_{gb}b - k_{db}b \quad (34)$$

in which

$$k_{gb}(i) = \frac{R_0(i)}{\bar{R}_0}\bar{k}_{gb}, \bar{R}_0 = \frac{1}{365}\sum_{i=1}^{365} R_0(i) \quad (35a)$$

and from Iqba (1983)

$$R_0(i) = 30 r_0(i)\left[\omega\frac{T_d(i)}{2}\sin\psi(i)\sin\lambda + \cos\psi(i)\cos\lambda\sin\left(\omega\frac{T_d(i)}{2}\right)\right]$$
$$r_0(i) = 1 + 0.033\cos\left(\frac{2\pi i}{365}\right)$$
$$\psi(i) = \sin^{-1}\left\{0.4\sin\left[\frac{2\pi}{365}(i - 82)\right]\right\}$$
$$T_d(i) = \frac{2\cos^{-1}(-\tan\psi(i)\tan(\Lambda))}{\omega} \quad (35b)$$

where k_{gb} is the growth rate parameter of rooted plants [T^{-1}]; k_{db} is the death rate of rooted plants [T^{-1}]; $\bar{k}_{gb}$ is the mean daily growth rate of rooted plants [d^{-1}]; $R_0(i)$ is solar radiation on day i; $r(i)$ is earth's eccentricity correction factor for day i; $T_d(i)$ is the total day length on day i; i is the day number of the year; Λ is latitude in radians; and ω is angular velocity of earth (15°/h, or $\pi/12$ rad/h).

Floating plants growth/death are described by this equation

$$\frac{da}{dt} = k_{ga}a - k_{da}a - \left(\frac{Q_o}{\phi_w V_w}\right)a \quad (36)$$

in which

$$k_{ga}(i) = \frac{R_0(i)}{\bar{R}_0}\bar{k}_{ga} \quad (37)$$

where k_{ga} is the growth rate parameter of a floating plant [T^{-1}]; k_{db} is the death rate of a floating plant [T^{-1}]; and $\bar{k}_{ga}$ is the mean daily plant growth rate for a floating plant [d^{-1}] (calibration parameter). The third term on the right-hand side accounts for the hydrologic export of floating biomass.

Diffusive Mass Transfer Coefficients

Expressions for the diffusive mass transfer coefficients β_a, β_n, and β_p can be obtained by conserving mass flow in the schematic two-layer system depicted in Fig. 3. Each layer has its unique thickness, l, porosity, ϕ, and diffusion coefficient, D. Assuming linear drop in concentration from the center of layer 1 to the interface separating the two layers, the mass flux of species C across the interface is $F_1 = \phi_1 D_1(C_1 - C_n)/(l_1/2)$. Similarly, for a linear drop in pore-water concentration from the interface to the center of layer 2, mass flux is $F_2 = \phi_2 D_2(C_n - C_2)/(l_2/2)$. The equivalent mass flux (from the center of layer 1 to the center of layer 2) is $F = \beta(C_1 - C_2)$. Conservation of mass requires $F_1 = F_2 = F$. An expression for C_n can be obtained from $F_1 = F_2$, which when substituted back into F_1 and equating the resulting expression to F, one obtains this expression for the effective diffusive mass transfer coefficient:

$$\beta = \frac{2\phi_1\phi_2 D_1 D_2}{\phi_2 D_2 l_1 + \phi_1 D_1 l_2}, \qquad D_i = \tau_i D^*, \qquad i = 1, 2 \quad (38)$$

J. Hydrol. Eng., 2013, 18(12): 1709-1723

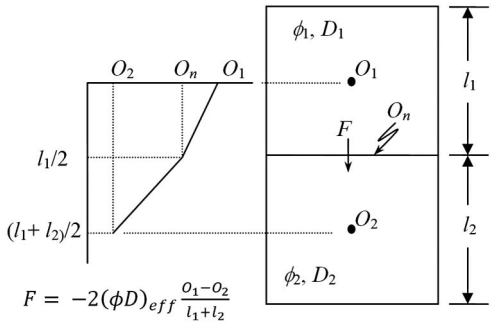

Fig. 3. Two porous cells and concept of effective diffusion parameter

where D^* is the free-water diffusion coefficient [L^2T^{-1}], and τ_i is tortuosity of layer i. For example, nitrate diffusive mass transfer from the water column (ϕ_w, h, D_n^*) to the aerobic soil layer (ϕ, l_1, D_n) is $\beta_{n1} = 2\phi_w\phi\tau D_n^*/(\phi\tau h + \phi_w l_1)$, where D_n and D_n^*, respectively, are nitrate soil and free-water diffusion coefficient [L^2T^{-1}]; and τ as defined above is the wetland soil tortuosity factor. Due to plant biomass and other debris obstructing flow, ϕ_w is generally less than 1 but expected to be larger than typical soil porosity.

Eq. (38) assumes linear variation of concentration between layers; however, for highly nonlinear concentration profiles, adjustment of β might be needed to compensate for potential errors.

Numerical Scheme Verification

Numerical integration was performed using an explicit scheme with forward-difference approximation of the time derivatives. The first-order ordinary differential equation (ODE) of each dependent variable C (constituent concentration or mass) in a particular compartment is cast in the form $dC/dt + \mu C = F$, where F denotes all sources and sinks including coupling terms (i.e., constituent variables coupled to C); and μ is the net sum of all constants/coefficients in the ODE multiplied by C. The time derivative is expressed using the forward-difference approximation $dC/dt \approx [C(t+\Delta t) - C(t)]/\Delta t$, with the second term on the left-hand side in the above ODE involving variable C approximated as $\mu(t+\Delta t)C(t+\Delta t)$. F is approximated with its value at the beginning of the time step, i.e., $F(t)$. Although the numerical scheme requires relatively small time increments Δt, it is essentially an explicit scheme, and the solution is straightforward and does not require solving a coupled system of equations.

The developed code was numerically verified using analytical solutions for simplified cases. Maple software [version 11 (Maplesoft, Waterloo, ON, Canada)] was used to obtain the analytical solutions. Simplifications were kept to a minimum in this process, i.e., the most complete sets of differential equations that have analytical solutions were used (available upon request). The model was run over a 2-year simulation time period using input data given in Tables 1–3 and mean parameter/coefficient values with prior distributions given in Table 4. The data in Tables 1–3 are obtained from a study on a restored treatment wetland (Jordan et al. 2003) described in Paper II. Table 4 lists model parameters, minima, maxima, and their prior distributions partly obtained from literature (related references are in Table 4 footnote) and partly expert judgment. The equations obtained by analytical solutions through Maple were too lengthy and are not shown here to conserve space. The time step Δt for the simulation was 1 day over the 2 years with the analytical solutions. The selected numerical integration time step is $\Delta t = 0.01$ day, but results were written at 1-day intervals for comparison purposes. The parameters were kept fixed for both numeric and analytic equations.

Table 1. Initial Concentrations (mg/L)

Parameter	Value
N_{ow}	1.80
N_{or}	0.91
N_{os}	0.14
a	0.04
b	0.05
m_w	36.0
N_{aw}	0.26
N_{a1}	0.09
N_{a2}	0.16
P_w	0.80
P_1	0.35
P_2	0.67
N_{nw}	0.40
N_{n1}	0.45
N_{n2}	0.43
m_s	0.30
O_w	6.0

Table 2. Hydrologic Variables

Parameter	Value
Q_i (m^3/day)	194.02
Q_o (m^3/day)	191.76
V_w (m^3)	2,409
A (m^2)	7,809
i_p (cm/day)	0.303
ET (cm/day)	0.332
l_1 (cm)	0.01
l_2 (m)	0.275

Table 3. Input Concentrations (mg/L)

Parameter	Value
N_{owi}	1.23
N_{nwi}	0.18
N_{awi}	0.12
P_{wi}	0.31
O_{wi}	6.011
m_{wi}	149.85
a^*	0.50
n^*	0.5
N_{nG}	0.056
N_{aG}	0.038
P_{wG}	0.01

Figs. 4–6 show almost perfect matches between analytical solutions and finite-difference solutions for organic nitrogen, total ammonia nitrogen, nitrate, and phosphorus in the water column and wetland soil. Differences between numerical and analytical solutions were indistinguishable in both oxidized and reduced soil layers for nitrate, total ammonia nitrogen, and phosphorus. Although not shown in figures, differences were negligible for organic nitrogen concentrations and free-floating and rooted plant biomass.

Sensitivity Analysis

In this section, we conducted a sensitivity analysis by perturbing all parameters and examined whether or not the mathematical model is

J. Hydrol. Eng., 2013, 18(12): 1709-1723

Table 4. Model Parameters Considered to Be Random

Notation	Unit	Min[a]	Max[a]	Distribution
l_2	cm	5	50	U
Λ	—	0.52	0.87	U
θ	—	1.0	1.2	U
K_d	mL/g	0.075	19.3	log-N
k_{ga}	1/day	0.01	0.2	log-N
k_{gb}	1/day	0.01	0.2	log-N
k_{ms}	1/day	0.000001	0.001	log-N
k_{nw}	1/day	0.0001	0.1	log-N
k_{mw}	1/day	0.000001	0.001	log-N
k_{ns}	1/day	0.01	10	log-N
k_{dn}	1/day	0.004	2.6	U
ρ_s	g/cm^3	1.5	2.2	U
v_s	cm/day	0.025	25	log-N
v_b	cm/day	0.000274	0.006575	U
a_{na}	gN/gChl	3.5	17.6	U
$r_{c,chl}$	gC/gChl	20	100	U
S_s	g/L/day	0.022	0.065	U
α	—	0.0864	0.3456	U
f_r	—	0.5	1	U
pK	—	4.3	12.9	U
pH	—	4.5	8.2	U
S	mg/m^2/day	0.0004	0.4	log-N
K_w	cm^3/g	10	100	log-N
a_{pa}	grP/grChl	0.4	2	U
D_{pw}	cm^2/day	0.66	0.83	U
K_{sa}	cm^3/g	10	100	log-N
K_{sb}	cm^3/g	100	1,000	log-N
ϕ	—	0.5	0.9	U
f_{Sw}	—	0.5	1	log-N
f_{ac}	—	20	1,000	log-N
v_r	mm/year	0.0146	8.74	log-N
K_0	cm/day	25.60	102.02	U
k_v	cm/day	14.64	23.10	U
f_N	—	0.00024	1.00	U
β_{a1}	cm/day	2.34	114.1	U
β_{n1}	cm/day	2.28	111.1	U
β_{p1}	cm/day	1.08	54.1	U

Note: U = uniform distribution; log-N = log-normal distribution. Lower and upper bounds in log-N distributions refer to values corresponding to probabilities of 0.1 and 99.9%.

[a]The selected range values for the listed parameters/coefficients are from soft information (i.e., literature tabulation and expert knowledge) (e.g., Kadlec and Knight 1996; Schnoor 1996; Chapra 1997; Di Toro 2001; Jørgensen and Bendoricchio 2001; Pivato and Raga 2006; Kalin and Hantush 2007; Liang et al. 2007; Reddy and Delaune 2008; and many other references). The range for some of the parameters was based on formulas presented in the main text.

performing adequately, as expected based on intuitive physical and biogeochemical system responses. We employed the Global Sensitivity Analysis (GloSA) technique (Haan 2002).

We generated 100,000 independent parameter sets by randomly sampling parameter values from the prior distributions listed in Table 4. Monte Carlo (MC) simulations were performed by running the model one parameter set at a time to yield 100,000 simulated output time series for each constituent concentration. In the GloSA technique, the statistical correlation between each of the sampled parameter values and corresponding MC model outputs is computed as outlined in Haan (2002). The correlation coefficients of each parameter at the end of the regression analysis are surrogate for each parameter's sensitivity. Both Pearson product moment correlation coefficient and Spearman's rank correlation coefficient (Saltelli and Sobol 1995; Quader and Guo 2009) were used in determining quantitatively the most sensitive parameters (Tables 5 and 6). The latter measures the degree of linear correlation between the ranks of each input and output rather than their absolute values. Therefore, Spearman's rank correlation really measures the strength of the monotonic relationship. A negative correlation implies that the computed variable is inversely related to the parameter.

In general, results shown in both tables are in agreement. Sediment is most sensitive to the settling and resuspension parameters, and much less to soil porosity. As expected, sediment concentration is negatively correlated with v_s and positively correlated with v_r. Increased settling velocity decreases sediment concentration in the water column and vice versa. On the contrary, a higher resuspension coefficient leads to higher sediment concentration.

Similar to sediment, particulate organic nitrogen (N_{ow}) is very sensitive and inversely related to v_s, as shown by the Pearson product moment correlation (−66%) and Spearman's rank correlation (−99%) (Tables 5 and 6). Both tables show no other sensitive parameters for N_{ow} next to v_s, not even k_{mw}, which controls the mineralization of organic nitrogen to ammonia.

For the particular initial concentrations and loading given in Tables 1–3, the fraction of total ammonia nitrogen concentration (N_{aw}) as NH_4^+ (f_N) appears to be the most sensitive parameter according to the Pearson product moment correlation coefficient (92%) and Spearman's rank correlation coefficient (87%). The high correlation with f_N can be partly attributed to the dominant role of NH_3 volatilization and NH_4^+ nitrification as major loss pathways for total ammonia nitrogen, and partly to adsorption of NH_4^+ onto sediment particles as a temporary buffer from further losses. A negative correlation with k_{nw} is consistent with a decreasing

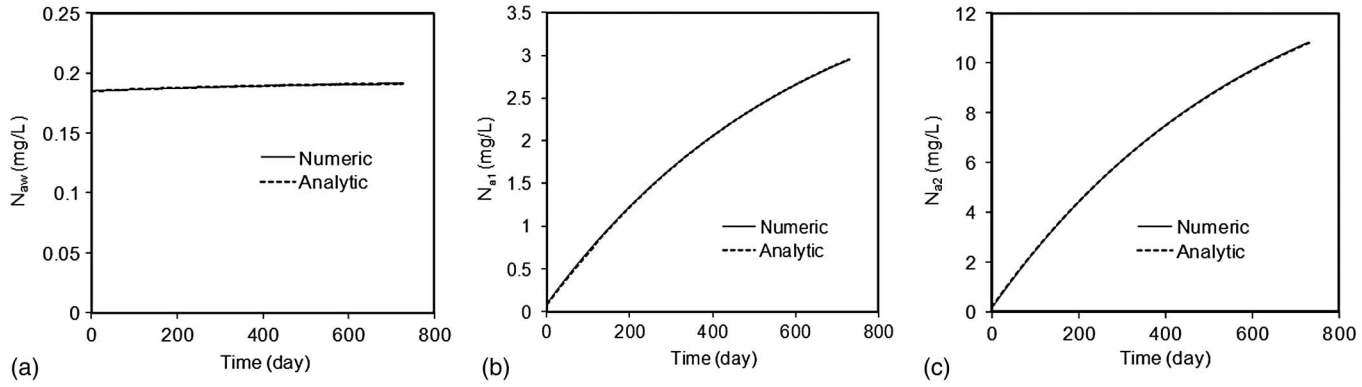

Fig. 4. Comparison of analytical and numerical simulations for total ammonia in (a) water column (N_{aw}); (b) aerobic soil layer (N_{a1}); (c) (N_{a2}) anaerobic soil layer

J. Hydrol. Eng., 2013, 18(12): 1709-1723

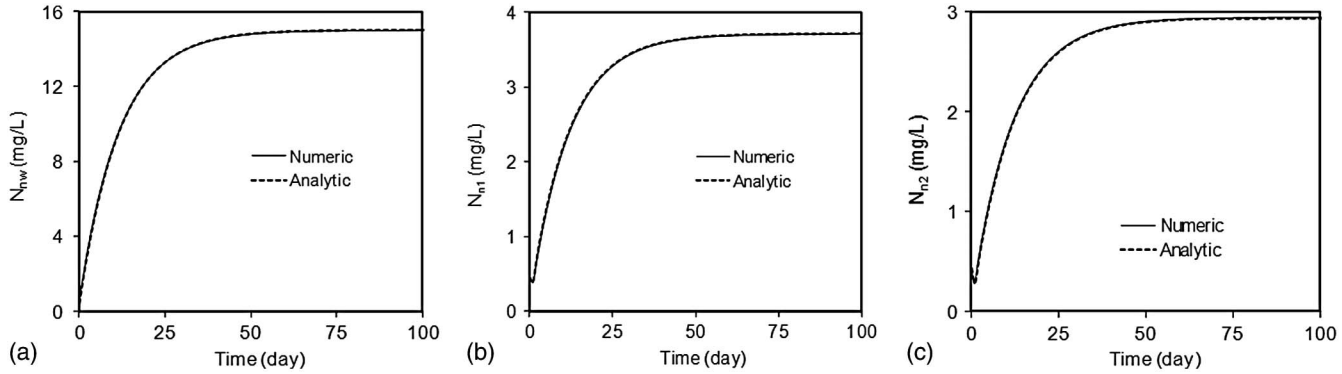

Fig. 5. Comparison of analytical and numerical simulations for nitrate in (a) water column (N_{nw}); (b) aerobic soil layer (N_{n1}); (c) anaerobic soil layer (N_{n2})

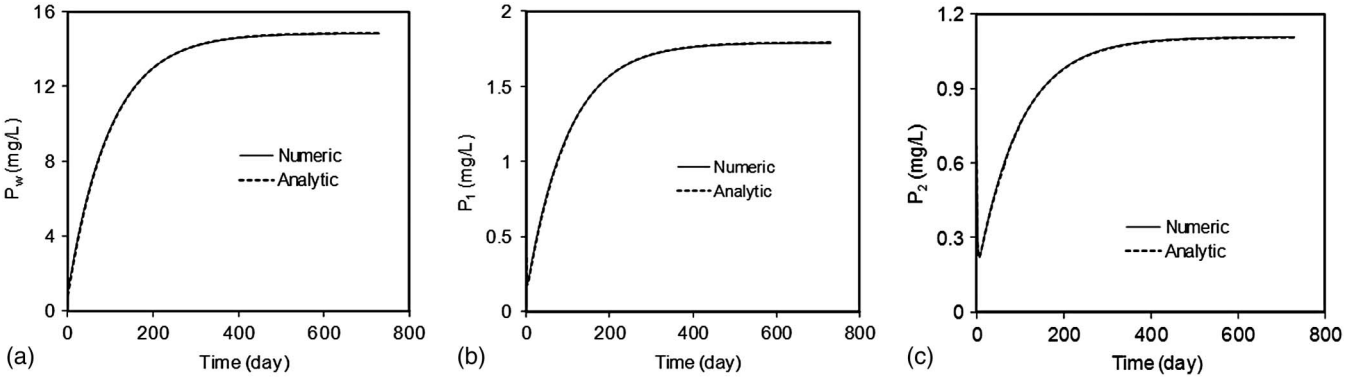

Fig. 6. Comparison of analytical and numerical simulations for phosphorous in (a) water column (P_w); (b) aerobic soil layer P_1; (c) anaerobic soil layer P_2

concentration of NH_4^+ with nitrification, and a positive correlation with k_{ms} is consistent with an increasing concentration of NH_4^+ with the mineralization process. An increasing nitrification rate results in substantial reduction in ammonia concentration, and a higher mineralization coefficient causes conversion of more organic nitrogen to mineral ammonium nitrogen. There is an apparent lack of correlation between N_{aw} and anaerobic layer thickness l_2, which for the scenario input concentrations in Table 3 is indicative of total ammonia nitrogen levels controlled by steady input to surface water, but with much less significant feedback from bottom sediments.

Table 5. Pearson Correlation Coefficients (%) of Model Outputs versus Model Parameters

Parameters	N_{ow} (%)	N_{aw} (%)	N_{nw} (%)	O_w (%)	P_w (%)	m_w (%)	N_{Tw} (%)
l_2	−0.1	0.1	−1.9	4.9	−60.1	4.0	−0.3
θ	−0.5	0.8	9.5	19.3	8.8	−0.6	0.9
K_d	−0.1	−0.7	−0.2	0.1	−0.2	0.1	−0.2
k_{ms}	−0.5	7.7	0.0	0.0	2.2	−0.2	1.2
k_{nw}	0.1	−7.7	7.2	0.1	0.0	0.0	−0.7
k_{ns}	−0.1	−0.8	0.0	−0.1	−0.1	0.0	−0.3
k_{dn}	−0.2	−0.2	−57.5	−0.3	0.0	0.2	−7.7
ρ_s	0.2	−0.2	−0.2	0.2	−13.7	5.3	0.2
v_s	−66.2	2.6	0.5	0.0	−1.4	−41.9	−63.9
S_s	−0.2	0.7	0.2	−31.1	0.4	−0.3	0.0
α	0.4	−3.2	0.7	76.9	−0.1	0.2	−0.2
K_w	−0.4	0.4	−0.5	−0.1	−47.3	−0.1	−0.3
ϕ	0.5	0.0	−9.3	−47.5	48.7	−13.7	−0.7
v_r	0.4	0.4	0.0	0.1	3.7	76.2	0.5
K_o	0.4	−3.2	0.7	76.9	−0.1	0.2	−0.2
f_N	−0.1	92.2	3.7	0.1	0.0	0.2	21.1
β_{a1}	—	−0.2	—	—	—	—	−6.0
β_{n1}	—	—	−47.6	—	—	—	−6.0
β_{p1}	—	—	—	—	−26.3	—	—

Table 6. Rank Correlation Coefficients (%) of Model Outputs versus Model Parameters

Parameters	N_{ow} (%)	N_{aw} (%)	N_{nw} (%)	O_w (%)	P_w (%)	m_w (%)	N_{Tw} (%)
l_2	−0.2	−1.0	0.9	4.7	−63.5	4.3	−0.4
θ	−0.4	1.5	9.9	18.8	7.7	−0.4	1.4
K_d	0.0	−3.0	−0.1	0.0	0.2	0.0	−0.2
k_{ms}	−0.2	13.8	−0.2	0.4	1.3	0.0	1.1
k_{nw}	−0.6	−20.0	5.0	0.5	−0.3	−0.4	−1.3
k_{dn}	0.2	−0.3	−55.3	−0.2	0.1	0.3	−9.2
ρ_s	0.4	−0.4	−0.4	0.3	−13.4	5.3	0.3
v_s	−99.5	8.0	0.3	0.1	−1.8	−77.2	−93.0
S_s	−0.1	1.4	0.1	−30.3	0.3	−0.2	0.1
α	−0.1	−6.6	0.7	76.8	−0.1	−0.1	−0.8
K_w	−0.2	0.3	−0.4	−0.1	−47.0	0.0	−0.3
ϕ	0.2	0.6	−11.5	−46.7	49.7	−13.6	−1.4
v_r	0.5	0.6	−0.1	−0.2	2.5	51.7	0.6
K_o	−0.1	−6.6	0.7	76.8	−0.1	−0.1	−0.8
f_N	−0.2	86.5	3.5	−0.2	−0.5	0.2	25.2
β_{a1}	—	−0.8	—	—	—	—	−9.1
β_{n1}	—	—	−65.4	—	—	—	−9.1
β_{p1}	—	—	—	—	−27.7	—	—

The relatively high negative correlations in both Pearson and Spearman rank correlations of nitrate concentrations (N_{nw}) with the denitrification rate (k_{dn}) and diffusive mass transfer coefficient (β_{n1}) are indicative of a strong decreasing trend with both parameters. Albeit smaller, the positive 7.2% correlation with k_{nw} reflects a monotonically increasing nitrate concentration with nitrification. As expected, higher denitrification rates reduce nitrate under reduced conditions in the soil, whereas higher nitrification rates increase the nitrate amount under aerobic conditions. The decrease of N_{nw} with β_{n1} is attributed to diffusive transport caused by concentration gradient from higher nitrate concentrations in the water column to lower concentrations in bottom soil, wherein nitrate is removed by denitrification under reduced condition. Although the anaerobic layer is where denitrification occurs, its thickness l_2 had a marginal impact on N_{nw}. As discussed above, external input seems to dominate sediment feedback in the given simulation scenario.

The last column in Tables 5 and 6 shows that total nitrogen concentration N_{Tw} is most sensitive to and negatively correlated with the settling velocity v_s. Both this correlation and the smaller one (in absolute value) with denitrification rate k_{dn} accentuate the role of settling into bottom sediments and denitrification therein as sinks for total nitrogen in the water column. At time scale of this example application, the model was not sensitive to burial velocity. However, it remains inconclusive whether or not burial is a long-term loss pathway.

Both Pearson and Spearman's rank correlations for total phosphorus (P_w) show large negative correlations with l_2 and K_w and high positive correlation with ϕ. This shows that for the given simulation scenario, settling and sorption onto soil particles is a removal process for total phosphorus in the water column. Positive correlations with k_{ms} and v_r are consistent with mineralization in bottom sediment and resuspension mechanism as sources for total phosphorus in the water column. Negative correlations also reveal significant inverse relationships between P_w and diffusive rate transfer coefficient (β_{p1}) and sediment particle density (ρ_s).

The negative correlations of dissolved oxygen in the water column (O_w) with S_s and φ in Tables 5 and 6 are expected because the increased oxygen removal rate in the sediment layer and larger sediment porosity lead to reduced oxygen levels in the water column. The large positive correlation with oxygen mass transfer rate (K_O) is also anticipated since O_w increases with the oxygen aeration rate.

The sensitivity analysis carried above points toward internal mathematics of the wetland model that are consistent with what is expected from various physical and biochemical processes. However, the order of parameter sensitivities is generally site-specific and might vary to some extent from one site to another, as parameters are surrogates of underlying physical and biogeochemical processes that can dominate under varying wetland conditions.

Phosphorus Precipitation/Release

In this section we attempted to simulate precipitation and release phenomena described above. The effect of oxygen level on phosphorus dynamics was simulated using Eq. (28). This relationship assumes maximum phosphorus adsorption when the water column is saturated with oxygen. The sorption coefficient decreases linearly when oxygen levels drop, thus resulting in more phosphorus in solution. In other words, $K_{s1} = K_{sa}$ when $O_w = 0$ and $K_{s1} = K_{sa} + K_{sb}$ when $O_w = O^*$.

To simulate these effects, a hypothetical scenario was constructed from two 5-day duration sediment and phosphorus input events that yielded low oxygen levels in the water column as shown in Fig. 7(a). This was done by exaggerating oxygen removal in wetland soil, S_o, by selecting an S_s value an order of magnitude higher than its mean value (0.044). The model then was run for 2 years with no further input following the hypothetical 10 days of loading events. Time zero in the figure corresponds to May 15. Note the low oxygen concentrations during warmer months (e.g., days 0–150, which corresponds to May 15 to October 15) and high oxygen levels in colder months (e.g., days 180–330, which corresponds

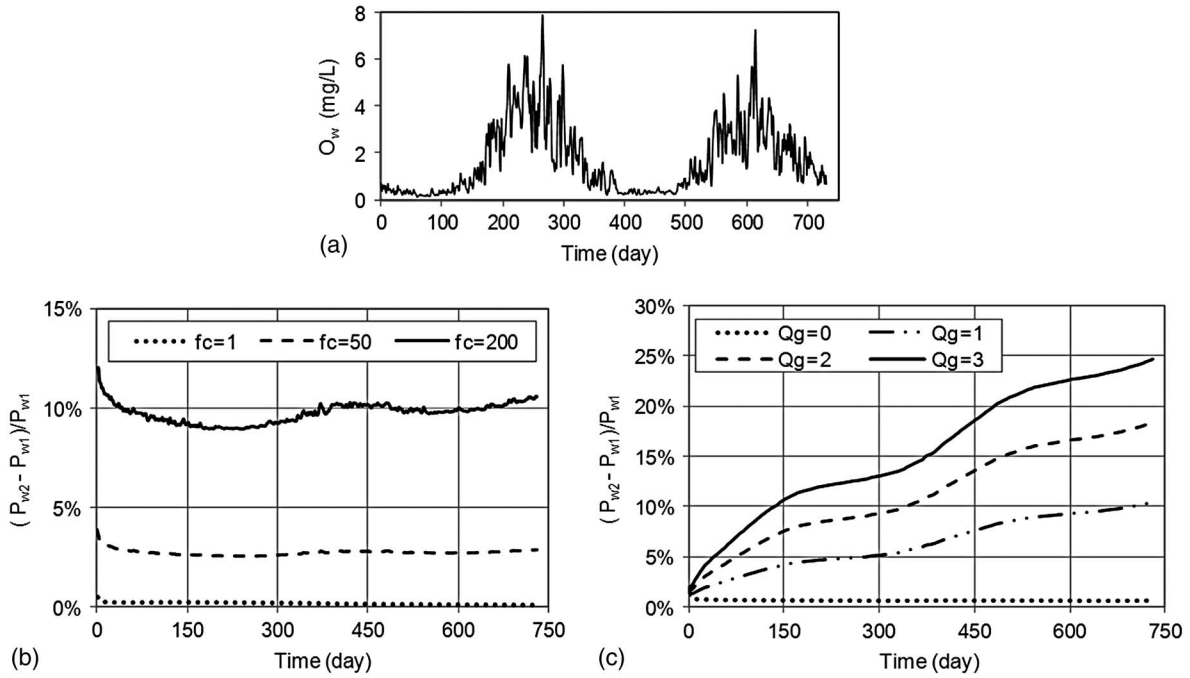

Fig. 7. Oxygen's effect on phosphorous concentration in the water; (a) a simulated scenario of water column oxygen concentrations; (b) the difference between P_w concentrations for cases 1 and 2 with a soil-water interface diffusion magnification effect; (c) the effect of groundwater discharge

J. Hydrol. Eng., 2013, 18(12): 1709-1723

to mid-December to mid-April). Two cases were considered. In the first case, the model was run ignoring the oxygen effect on phosphorus sorption onto sediment particles. In other words, K_{s1} was assumed at its maximum $K_{sa} + K_{sb}$ all the time regardless of variation in oxygen. In the second case, the model was run considering variation of K_{s1} with O_w using Eq. (28). If the model is capable of capturing the phenomenon described above, then we should expect to see higher phosphorus concentrations with case 2.

Figs. 7(b and c), respectively, show the differences in simulated phosphorus concentrations under different values of diffusion magnification factor f_{ac} and varying groundwater discharge rates Q_g. Phosphorus diffusion across the soil-water interface is magnified by multiplying the free-water diffusion coefficient by f_{ac} to simulate the effect of wind-induced turbulence and bioturbation. It is clearly seen that simulations with case 2 generated higher dissolved phosphorus concentrations in the water column. Considering molecular diffusion only (without turbulence/bioturbation and groundwater discharge) showed marginal differences between the two cases. If the diffusion coefficient increases by an order of magnitude or more, one can observe significant differences between the two scenarios [Fig. 7(b)]. Simulated dissolved phosphorus concentrations in the water column are greater for the second scenario with periodic decrease and increase in the computed concentrations coinciding, respectively, with periods of high and low dissolved oxygen [compare Fig. 7(a) with Fig. 7(b)]. The smallest difference is around the 250th day, on which day the oxygen concentration is highest. The peaks are at around the 75th and 450th days and at the end of the simulation, which all coincide with low oxygen levels.

This behavior is either dampened or accentuated by the mode of groundwater and surface water interactions. Higher groundwater discharge rates (m/d) (effluent wetlands) magnify the difference [Fig. 7(c)]. Although not shown in a figure, infiltration (i.e., influent wetlands) diminishes the mechanism of phosphorus release during low oxygen periods by countering the effect of upward diffusive migration to the water column. Worth noting also is that the slope of the relative differences between the two scenarios is steeper during the periods of low oxygen (e.g., days 0–150) than during periods with higher oxygen levels (e.g., days 180–330), as Fig. 7(c) shows.

Summary and Conclusions

Wetlands are recognized for controlling floods and providing water quality and ecological benefits. In this part of a two-paper series, using basic physical and biochemical principles, a process-based mathematical model has been developed using conservation of mass to simulate nutrient retention, cycling, and removal in flooded wetlands. Specifically, transport and fate of organic and inorganic nitrogenous and phosphorus constituents in the water column and wetland soil are emphasized. The role of primary productivity on nutrient cycling is accounted for in an aggregate manner, but without a plant diversity component and shading and growth relationship. The novel aspect of this development, however, is the model ability to simulate with relative ease oxygen dynamics in the wetland system and the formation of a thin, oxidized surface layer that exerts geochemical control on nitrogen and phosphorus cycling at the soil-water interface. The model accounts for nitrogen loss by ammonia volatilization as a function of environmental factors and a newly derived volatilization rate transfer coefficient. The process of precipitation of insoluble phosphate under aerobic conditions and release into solution under anoxic conditions was also modeled by proposing a functional relationship between sorption coefficient and oxygen concentration.

The coupled system of ordinary differential equations is solved using the finite-difference method. Comparison with analytical solutions of specific scenarios revealed the adequacy of the numerical scheme. Global sensitivity analysis revealed the order of parameter sensitivities that is generally anticipated and consistent with the wetland sediment and nutrient loading scenario application.

Application to a hypothetical phosphorus loading scenario illustrated the conditions where the wetland model was capable of capturing the phenomenon of orthophosphate precipitation under aerobic conditions and releases into solution under anoxic conditions.

The limitations of this model nonetheless should be recognized from the underlying assumptions, and further improvements are warranted. The most notable areas of additions include unsaturated conditions, transverse-lateral interactions with stagnant zones, extension to carbon cycling, and coupling of dissolved organic carbon to nitrogen transformation. Other areas needing improvement include adding microbial-communities dynamics and improving the primary productivity component. The model, however, is robust, and spatial variability along the main flow direction can be accounted for in a straightforward fashion. The wetland nutrient model is a potential tool for the design and management of constructed and natural wetlands.

Appendix I. Ammonia Volatilization Mass Transfer Velocity

From Whitman's two-film resistance model, one can show that net transfer velocity of any gas across the air-water interface is given by (Chapra 1997)

$$k_v = K_l \frac{H_e}{H_e + R_G T_a (K_g/K_l)} \,(\mathrm{m\,d^{-1}}) \tag{39}$$

where K_l = mass-transfer velocity in the liquid laminar layer ($\mathrm{m\,d^{-1}}$); K_g = mass transfer velocity in the gaseous laminar layer ($\mathrm{m\,d^{-1}}$); H_e = Henry's constant (1.37×10^{-5} $\mathrm{atm\,m^3\,mole^{-1}}$ at 20°C for NH_3); R_G = universal gas constant (8.206×10^{-5} $\mathrm{atm\,m^3\,(K^{-1}mole^{-1})}$; and T_a = absolute temperature (K).

The liquid-film and gaseous-film exchange can be calculated as a function of molecular weight and the corresponding coefficients for oxygen and water vapor (Jørgensen and Bendoricchio 2001)

$$K_l = K_{l,\mathrm{O_2}} \left(\frac{32}{M}\right)^{0.25} \tag{40}$$

and

$$K_g = K_{l,\mathrm{H_2O}} \left(\frac{18}{M}\right)^{0.25} \tag{41}$$

where $K_{l,\mathrm{O_2}}$ = liquid-film exchange coefficient for oxygen; and $K_{l,\mathrm{H_2O}}$ = gaseous-film exchange coefficient for water vapor. The gas-film coefficient for water can be approximated by (e.g., Chapra 1997; Jørgensen and Bendoricchio 2001)

$$K_{l,\mathrm{H_2O}} = 168 U_w \tag{42}$$

where U_w = wind speed ($\mathrm{m\,s^{-1}}$); and $K_{l,\mathrm{H_2O}}$ is in units ($\mathrm{m\,d^{-1}}$). We assume the following power relationship relating liquid-film mass transfer coefficient to wind speed:

$$K_{l,\mathrm{O_2}} = \alpha U_w^{\eta} \tag{43}$$

where α and η are empirical parameters. Combining (43) and (42) with (41) and (42) and substituting into (39) yields

J. Hydrol. Eng., 2013, 18(12): 1709-1723

$$k_v = \frac{1.17\alpha}{1 + 12.07\alpha U_w^{\eta-1}} U_w^{\eta} \tag{44}$$

Appendix II. Temperature-Dependent Coefficients

In general, reaction rates and physiological parameters vary with temperature in natural water environments. Assuming temperature variations over narrow ranges (e.g., 0 to 35°C), the Arrhenius equation could be used to derive this parameter-temperature formula (e.g., Schnoor 1996):

$$k_T = k_{20}\theta^{T-20} \tag{45}$$

where T = temperature expressed in °C; θ = constant temperature coefficient greater than 1.0 and usually within the range 1.0 to 1.10; and k_{20} = rate constant at the reference temperature 20°C. For example, Chapra (1997) recommended $\theta \cong 1.024$ for oxygen mass-transfer coefficient, K_O.

This temperature variation formula might be applicable to reaction-related and plant-related rate parameters k_{da}, k_{db}, k_{mw}, k_{mr}, k_{ms}, k_{nw}, k_{ga}, k_{gb}, k_{ns}, and k_{dn}. We also extend Eq. (45) to describe temperature variation of nitrogen fixation, S, and soil oxygen consumption rate parameters, S_w and S_s.

The dependence of oxygen saturation, O^*, on temperature may be described by the following relationship (Chapra 1997; refer to Jørgensen and Bendoricchio 2001, on modification for chlorination):

$$O^* = \exp\left(-139.34411 + \frac{1.575701 \times 10^5}{T_a} - \frac{6.642308 \times 10^7}{T_a^2} + \frac{1.2438 \times 10^{10}}{T_a^3} - \frac{8.621949 \times 10^{11}}{T_a^4}\right) \tag{46}$$

where O^* = saturation concentration of dissolved oxygen in fresh water at 1 atm (mg L^{-1}); and $T_a = T + 273.15$ is absolute temperature in °K. Chapra (1997) provides a correction to this equation for salinity and pressure effects.

The fraction of total ammonia in ionized form, f_N, is related to both temperature and pH using a relationship originally proposed by Emerson et al. (1975):

$$f_N = \frac{10^{-pH}}{10^{-pH} + \exp(-2.3026pK)}, \quad pK = \left(c_1 + \frac{c_2}{T_a}\right) \tag{47}$$

where c_1 and c_2 ($\approx$ 0.09018 and 2729.92, respectively, Emerson et al. 1975) might be treated as calibration parameters.

Boudreau (1997) provides these temperature-dependent free-water diffusion coefficients in units of ($cm^2 d^{-1}$) for oxygen, D_o^*, ammonium ion (D_a^*), and nitrate (D_n^*):

$$D_o^* = 0.864\left(0.2604 + 0.006383\frac{T}{\mu}\right) \tag{48}$$

$$D_a^* = 0.0864(9.5 + 0.413T) \tag{49}$$

$$D_n^* = 0.0864(9.5 + 0.388T) \tag{50}$$

and an average equation for inorganic phosphorus (PO_4^{3-}, HPO_4^{2-}, $H_2PO_4^-$) free-water diffusion coefficient (D_p^*) in units of ($cm^2 d^{-1}$) takes the form

$$D_p^* = 0.0864(3.3 + 0.181T) \tag{51}$$

where T is in °C [°K in (48)]; and μ = dynamic viscosity of water in centipoises (10^{-2} g $cm^{-1} s^{-1}$). A relationship relating μ in centipoises to T in (°C) can be obtained by fitting μ to T values reported by Chapra (1997):

$$\mu = 0.5e^{-0.0762T} + 1.3e^{-0.0177T} \tag{52}$$

A more general relationship relating μ to temperature, salinity, and pressure developed by Matthaus (as cited by Boudreau 1997) could also be used.

Acknowledgments

The U.S. Environmental Protection Agency through its Office of Research and Development partially funded and collaborated in the research described here under contract (EP08C000066) with Auburn University, School of Forestry and Wildlife Sciences. It has not been subject to the Agency review and therefore does not necessarily reflect the views of the Agency, and no official endorsement should be inferred.

Notation

The following symbols are used in this paper:

a_{na} = gram of nitrogen per gram of chlorophyll-a in plant/algae;
a_{oc} = gram of oxygen produced per gram of organic carbon synthesized (= 2.67);
a_{pa} = gram of phosphorus per gram of chlorophyll-a;
a_{pn} = phosphorus-to-nitrogen mass ratio produced by mineralization of particulate organic matter (POM) (= 1.389);
f_{aw} = fraction of mineral nitrogen plant uptake as ammonia-N in free water;
f_{a1} = fraction of mineral nitrogen plant uptake as ammonia-N in the soil aerobic layer;
f_{a2} = fraction of mineral nitrogen plant uptake as ammonia-N in the soil anaerobic layer;
f_{bs} = fraction of rooted plant biomass below soil-water interface (within soil layer);
f_{bw} = fraction of rooted plant biomass above soil-water interface;
f_N = fraction of total ammonia nitrogen ($[NH_4^+] + [NH_3]$) as NH_4^+;
f_{nw} = fraction of mineral nitrogen plant uptake as nitrate-N in free water;
f_{n1} = fraction of mineral nitrogen plant uptake as nitrate-N in the aerobic layer;
f_{n2} = fraction of mineral nitrogen plant uptake as nitrate-N in the anaerobic layer;
f_r = fraction of rapidly mineralizing particulate organic matter;
f_{Sw} = fraction of nitrogen fixation in water;
f_s = fraction of slowly mineralizing particulate organic matter;
f_1 = volumetric fraction of the active soil layer that is aerobic;
f_2 = volumetric fraction of the active soil layer that is anaerobic;
K_d = ammonium ion distribution coefficient [$L^3 M^{-1}$];
K_o = oxygen reaeration mass-transfer velocity [LT^{-1}];
k_{da} = death rate of free-floating plants [T^{-1}];
k_{db} = death rate of benthic and rooted plants [T^{-1}];
k_{dn} = denitrification rate in anaerobic soil layer [T^{-1}];
k_{ga} = growth rate of free-floating plant [T^{-1}];
k_{gb} = growth rate of benthic and rooted plant [T^{-1}];
k_{mr} = first-order rapid mineralization rate in wetland soil [T^{-1}];
k_{ms} = first-order slow mineralization rate in wetland soil [T^{-1}];

J. Hydrol. Eng., 2013, 18(12): 1709-1723

k_{mw} = first-order mineralization rate in wetland free water [T^{-1}];
k_{ns} = first-order nitrification rate in aerobic soil layer [T^{-1}];
k_{nw} = first-order nitrification rate in wetland free water [T^{-1}];
k^*_{nw} = maximum first-order nitrification rate in wetland free water [T^{-1}];
k^*_s = maximum first-order nitrification rate in wetland soil [T^{-1}];
k_v = volatilization mass transfer velocity [LT^{-1}];
$r_{c,chl}$ = carbon mass ration in chlorophyll a;
$r_{on,m}$ = gram of oxygen consumed per gram of organic nitrogen mineralized (= 15.29);
$r_{on,n}$ = gram of oxygen consumed per gram of total ammonium nitrogen nitrified (= 4.57);
α, η = empirical parameters in Eq. (7) for ammonia liquid-film transfer velocity;
β_{a1}, β_{n1} = diffusive mass-transfer rates, respectively, of total ammonia nitrogen and nitrate between wetland water and aerobic soil layer [LT^{-1}];
β_{a2}, β_{n2} = diffusive mass-transfer rates, respectively, of total ammonia nitrogen and nitrate between aerobic and anaerobic soil layers [LT^{-1}];
β_{p1} = diffusive mass-transfer rate of dissolved phosphorus between wetland water and aerobic soil layer [LT^{-1}];
β_{p2} = diffusive mass-transfer rate of dissolved phosphorus between aerobic and anaerobic soil layers [LT^{-1}]; and
λ_s, λ_w = empirical coefficients in the relationships limiting nitrification, respectively, in soil and free water to oxygen concentration in wetland water.

References

Bodkin, D. B., Janak, J. F., and Wallis, J. R. (1972). "Some ecological consequences of a computer model of forest growth." *J. Ecol.*, 60(3), 849–872.

Boudreau, B. P. (1997). *Diagenetic models and their implementation: Modeling transport and reactions in aquatic sediments*, Springer, Berlin, Heidelberg, 414.

Broecker, H. C., Petermann, J., and Siems, W. (1978). "The influence of wind on CO_2 exchange in a wind-wave tunnel." *J. Marine Res.*, 36(4), 595–610.

Brown, L. C., and Barnwell, T. O., Jr. (1987). "The enhanced stream water quality models QUAL2E and QUAL2E-UNCAS: Documentation and User Manual." *Report EPA/600/3-87/007*, U.S. Environmental Protection Agency, Athens, GA.

Brown, M. T. (1988). "A simulation model of hydrology and nutrient dynamics in wetlands." *Comput. Environ. Urban Syst.*, 12(4), 221–237.

Brown, S. L. (1981). "A comparison of the structure, primary productivity, and transpiration of cypress ecosystems in Florida." *Ecol. Monogr.*, 51(4), 403–427.

Buresh, R. J., Reddy, K. R., and van Kessel, C. (2008). "Nitrogen transformations in submerged soils." *Agronomy*, 49, 401–436.

Chapra, S. C. (1997). *Surface water-quality modeling*, McGraw-Hill, New York.

Di Toro, D. M. (2001). *Sediment flux modeling*, Wiley, New York.

Emerson, K., Russo, R. C., Lund, R. E., and Thurston, R. V. (1975). "Aqueous ammonia equilibrium calculations: Effect of pH and temperature." *J. Fish. Res. Board. Can.*, 32(12), 2379–2383.

Faulkner, S. P., and Richardson, C. J. (1989). "Physical and chemical characteristics of fresh-water wetland soils." In *Constructed wetlands for wastewater treatment, municipal, industrial and agricultural*, D. A. Hammer, ed., Lewis Publishers, Boca Raton, FL, 41–72.

Haan, C. T. (2002). *Statistical methods in hydrology*, 2nd Ed., Iowa State Press.

Hammer, D. A. (1989). "Wetland ecosystems: Natural water purifiers?" *Constructed wetlands for wastewater treatment, municipal, industrial and agricultural*, D. A. Hammer, ed., Lewis Publishers, Boca Raton, FL, 5–19.

Hantush, M. M. (2007). "Modeling nitrogen-carbon cycling and oxygen consumption in bottom sediments." *Adv. Water Resour.*, 30(1), 59–79.

Iqba, M. (1983). *An introduction to solar radiation*, Academic Press, New York.

Jordan, T. E., Whigham, D. F., Hofmockel, K. H., and Pittek, M. A. (2003). "Nutrient and sediment removal by a restored wetland receiving agricultural runoff." *J. Environ. Qual.*, 32, 1534–1547.

Jørgensen, S. E., and Bendoricchio, G. (2001). *Fundamentals of ecological modeling*, 3rd Ed., Elsevier, New York.

Jørgensen, S. E., Hoffman, C. C., and Mitsch, W. J. (1988). "Modeling nutrient retention by Reedswamp and wet meadow in Denmark." *Wetland modeling*, W. J. Mitsch, M. Straškraba, and S. E. Jørgensen, eds., Elsevier, New York, 133–152.

Kadlec, R. H. (1989). "Decomposition in wastewater wetlands." *Constructed wetlands for wastewater treatment, municipal, industrial and agricultural*, D. A. Hammer, ed., Lewis Publishers, Boca Raton, FL, 459–468.

Kadlec, R. H. (1997). "An autobiotic wetland phosphorus model." *Ecol. Eng.*, 8(2), 145–172.

Kadlec, R. H., and Hammer, D. A. (1988). "Modeling nutrient behavior in wetlands." *Ecol. Modell.*, 40(1), 37–66.

Kadlec, R. H., and Knight, R. L. (1996). "*Treatment Wetlands*, Lewis Publishers, 459.

Kalin, L., and Hantush, M. M. (1996). "Predictive uncertainty and parameter sensitivity of a sediment-flux model: Nitrogen flux and sediment oxygen demand", *World Environment and Water Resources Congress: Restoring Our Natural Habitat*, Tampa, May 15–19.

Kalin, L., Hantush, M. M., Isik, S., Yucekaya, A., and Jordan, T. (2013). "Nutrient dynamics in flooded wetlands. II: Model application." *J. Hydrol. Eng.*, 10.1061/(ASCE)HE.1943-5584.0000750, 1724–1738.

Kirk, G. J. D., and Kronzucker, H. J. (2005). "The potential for nitrification and nitrate uptake in the rhizosphere of wetland plants: A modeling study." *Ann. Bot.*, 96(4), 639–646.

Langergraber, G. (2001). "Development of a simulation tool for subsurface flow constructed wetlands." Wiener Mitteilungen 169, Vienna, Austria, P. 207.

Langergraber, G., Rousseau, D. P. L., Garcia, J., and Mena, J. (2009). "CWM1: A general model to describe biokinetic processes in subsurface flow constructed wetlands." *Water Sci. Technol.*, 59(9), 1687–1697.

Liang, X. Q., et al. (2007). "Modeling transport and fate of nitrogen from urea applied to a near-trench paddy field." *Environ. Pollut.*, 150(3), 13–320.

Logofet, D. O., and Alexandrov, G. A. (1988). "Interference between mosses and trees in the framework of a dynamic model of carbon and nitrogen cycling in a mesotrophic bog ecosystem." *Wetland modeling*, W. J. Mitsch, M. Straškraba, and S. E. Jørgensen, eds., Elsevier, New York, 55–66.

Min, J.-H., Paudel, R., and Yawitz, J. W. (2011). "Mechanistic biogeochemical model applications for Everglades restoration: A review of case studies and suggestions for future modeling needs." *Crit. Rev. Env. Sci. Technol.*, 41(S1), 489–516.

Mitsch, W., Straškraba, M., and Jørgensen, S. E. (1988). "Wetland modeling—An introduction and overview." *Wetland modeling*, W. J. Mitsch, M. Straškraba, and S. E. Jørgensen, eds., Elsevier, New York, 1–8.

Mitsch, W. J., and Gosselink, J. G. (2000). *Wetland*, Wiley, New York.

Mitsch, W. J., and Reeder, B. C. (1991). "Modeling nutrient retention of a freshwater coastal wetland: Estimating the roles of primary productivity, resuspension and hydrology." *Ecol. Modell.*, 54(3–4), 151–187.

Odum, E. P. (1979). "Ecological importance of the riparian zone." *Strategies for protection and management of floodplain wetlands and other riparian ecosystems*, R. R. Johnson and J. F. McCormick, eds., Forest Service General Technical Report WO-12, Washington, DC, 2–4.

Paudel, R., and Jawitz, J. W. (2012). "Does increased model complexity improve description of phosphorus dynamics in a large treatment wetland?" *Ecol. Eng.*, 42, 283–294.

Paudel, R., Min, J.-H., and Jawitz, J. W. (2010). "Management scenario evaluation for a large treatment wetland using a spatio-temporal phosphorus transport and cycling model." *Ecol. Eng.*, 36(12), 1627–1638.
Pearlstein, L., McKellar, H., and Kitchens, W. (1985). "Modelling the impact of a river diversion on bottomland forest communities in the Santee River floodplain, South Carolina." *Ecol. Modell.*, 29(1–4), 283–302.
Phipps, R. L. (1979). "Simulation of wetlands forest vegetation dynamics." *Ecol. Modell.*, 7(4), 257–288.
Pivato, A., and Raga, R. (2006). "Tests for the evaluation of ammonium attenuation in MSW landfill leachate by adsorption into bentonite in a landfill liner." *Waste Manage.*, 26(2), 123–132.
Quader, A., and Guo, Y. (2009). "Relative importance of hydrological and sediment-transport characteristics affecting effective discharge of small urban streams in southern Ontario." *J. Hydrol. Eng.*, 10.1061/(ASCE)HE.1943-5584.0000042, 698–710.
Raghunathan, R., et al. (2001). "Exploring the dynamics and fate of total phosphorus in the Florida Everglades using a calibrated mass balance model." *Ecol. Modell.*, 142(3), 247–259.
Reddy, K. A., and Delaune, R. D. (2008). *Biogeochemistry of wetlands: Science and applications*, CRC Press, Boca Raton, FL.
Reddy, K. R., and Patrick, W. H. (1984). "Nitrogen transformations and loss in flooded soils and sediments." *Crit. Rev. Environ. Control*, 13(4), 273–309.
Reed, S. C., Middlebrooks, F. J., and Crites, R. W. (1988). *Natural systems for waste management and treatment*, McGraw-Hill, New York.
Saltelli, A., and Sobol, I. M. (1995). "About the use of rank transformation in sensitivity analysis of model output." *Reliab. Eng. Syst. Saf.*, 50(3), 225–239.
Schnoor, J. L. (1996). *Environmental modeling: Fate and transport of pollutants in water, air, and soil*, Wiley, New York.
Thoman, R. V., and Mueller, J. A. (1987). *Principles of surface water quality modeling and control*, HarperCollins, London.
Van der Peijl, M. J., and Verhoeven, J. T. A. (1999). "A model of carbon, nitrogen and phosphorus dynamics and their interactions in river marginal wetlands." *Ecol. Modell.*, 118(2–3), 95–130.
Walker, W. W. (1995). "Design basis for Everglades stormwater treatment areas." *Water Res. Bullet.*, 31, 671–685.
Walker, W. W., and Kadlec, R. H. (2011). "Modeling phosphorus dynamics in Everglades wetlands and stormwater treatment areas." *Crit. Rev. Env. Sci. Technol.*, 41(S1), 430–446.
Wang, N., and Mitsch, W. J. (2000). "A detailed ecosystem model of phosphorus dynamics in created riparian wetlands." *Ecol. Modell.*, 126(2–3), 101–130.
Wang, Y., et al. (2009). "A simulation model of nitrogen transformation in reed constructed wetlands." *Desalination*, 235(1–3), 93–101.
Water Quality Institute (VKI). (1992). *MIKE 11 WET, short description*, VKI, Hørsholm, Denmark.
Watson, J. T., Reed, S. C., Kadlec, R. H., Knight, R. L., and Whitehouse, A. E. (1989). "Performance expectations and loading rates for constructed wetlands." *Constructed wetlands for wastewater treatment, municipal, industrial and agricultural*, D. A. Hammer, ed., Lewis Publishers, Boca Raton, FL, 319–351.